Developmental Cell

Supplemental Information

A Family of Tetraspans Organizes Cargo for Sorting into Multivesicular Bodies

Chris MacDonald, Johanna A. Payne, Mariam Aboian, William Smith, David J. Katzmann, Robert C. Piper

Supplemental Figure 1

a

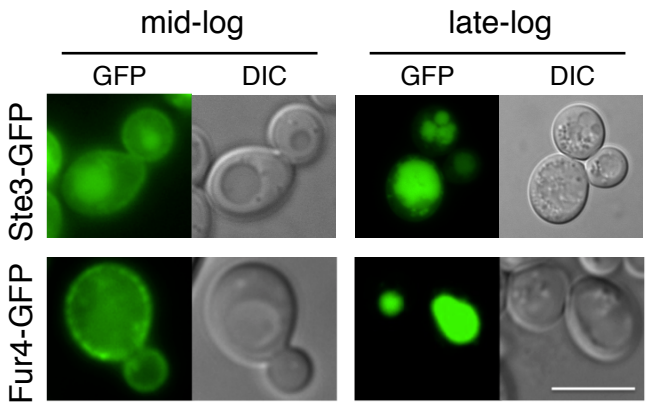

bsd2Δ art1Δ art2Δ art3Δ art4Δ art6Δ art7Δ art8Δ art10Δ

b

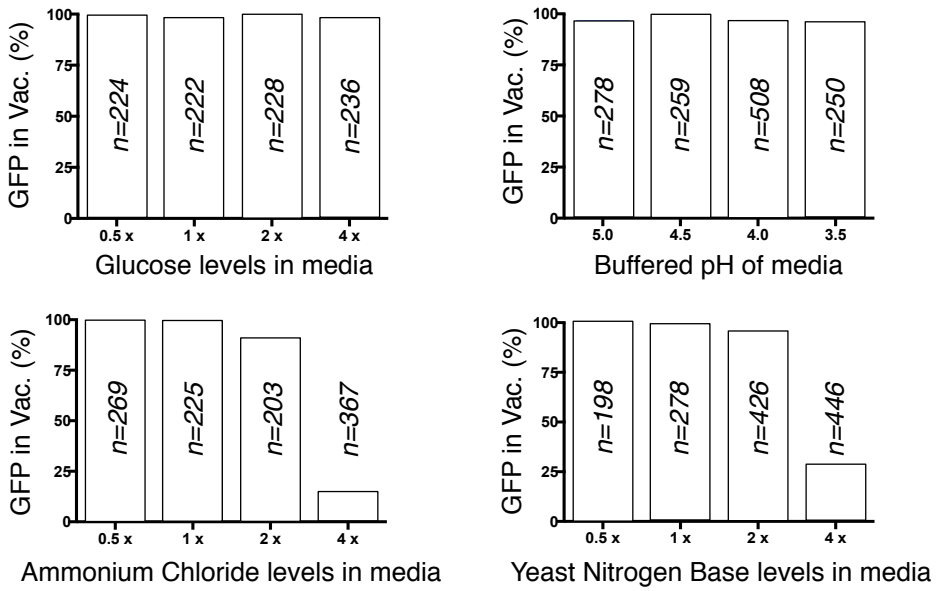

c

VITAMINS
Thiamine HCl (B1), 1.5μM
Riboflavin (B2), 0.5μM
Niacin (B3), 3.2μM
Calcium pantothenate (B5), 8μM
Pyridoxine HCl (B6), 2.3μM
Biotin (B7), 8nM
Inositol (B8), 11μM
Folic acid (B9), 4nM
p-Aminobenzoate (Bx), 3μM

SALTS
H_3BO_3, 8μM
$CuSO_4$, 0.25μM
KI, 0.6μM
$FeCl_3$, 1.2μM
$MgSO_4$, 2.6μM
Na_2MoO_4, 1μM
$ZnSO_4$, 2.4μM
KH_2PO_4, 7.3mM
$MgSO_4$, 4.1mM
NaCl, 1.7mM
$CaCl_2$, 0.9mM

d

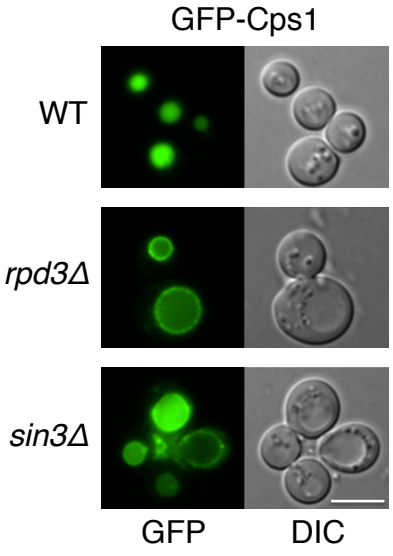

Supplemental Figure 2

a

Hours after log phase

	2	4	8	12
COS1	0.48	0.44	1.45	1.92
COS2	0.21	0.37	1.06	1.67
COS3	0.44	0.64	1.48	2.24
COS4	0.59	0.96	1.77	2.21
COS5	0.36	0.76	1.00	2.18
COS6	0.57	0.79	1.62	2.07
COS7	0.12	0.09	0.89	1.17
COS8	0.50	0.79	1.30	2.16
COS9	0.28	0.53	1.03	1.07
COS10	0.01	0.24	0.20	-0.22
COS12	-0.14	0.16	-0.20	0.78
Average	0.31	0.52	1.05	1.57

Deletion of HDACs

	rpd3Δ	*sin3Δ*	*hda1Δ*	*sir2Δ*
COS1	-2.30	-2.20	0.02	0.40
COS2	-2.24	-2.21	0.11	0.49
COS3	-2.66	-2.44	0.03	0.43
COS4	-2.24	-2.01	0.02	0.52
COS5	-2.57	-2.39	0.06	0.53
COS6	-2.37	-2.39	0.18	0.54
COS7	-2.66	-2.55	0.33	0.51
COS8	-2.55	-2.36	0.08	0.53
COS9	-2.54	-2.36	0.32	-0.02
COS10	0.87	0.37	0.64	-0.11
COS12	-3.29	-2.56	-0.73	3.58
Average	-2.23	-2.10	0.09	0.67

Repression — Induction

b

AAD13 / YNL331C Putative aryl-alcohol dehydrogenase;
COS1 / YNL336W Protein of unknown function; member of the DUP380 subfamily
COS2 / YBR302C Protein of unknown function; member of the DUP380 subfamily
COS3 / YML132W Protein of unknown function; member of the DUP380 subfamily
COS4 / YFL062W Protein of unknown function; member of the DUP380 subfamily
COS5 / YJR161C Protein of unknown function; member of the DUP380 subfamily
COS6 / YGR295C Protein of unknown function; member of the DUP380 subfamily
COS7 / YDL248W Protein of unknown function; member of the DUP380 subfamily
COS8 / YHL048W Protein of unknown function; member of the DUP380 subfamily
YIR043C Pseudogene related to COS proteins
HSP31 / YDR533C Methylglyoxalase
RTC2 / YBR147W vacuolar transporter for cationic amino acids
SHH3 / YMR118C Putative mitochondrial inner membrane protein of unknown function
SRY1 / YKL218C 3-hydroxyaspartate dehydratase;
YNR071C Putative aldose 1-epimerase

c

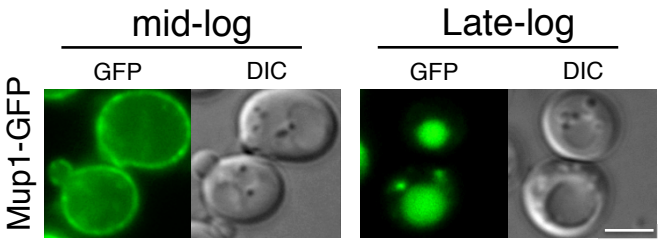

hda1Δ

d

Percent Identity

	protein	gene
Cos5	--	--
Cos7	94	96
Cos1	87	93
Cos2	86	93
Cos3	86	93
Cos4	84	87
Cos6	81	84
Cos8	76	86
Cos9	62	47
Cos10	44	37
Cos12	40	35

e

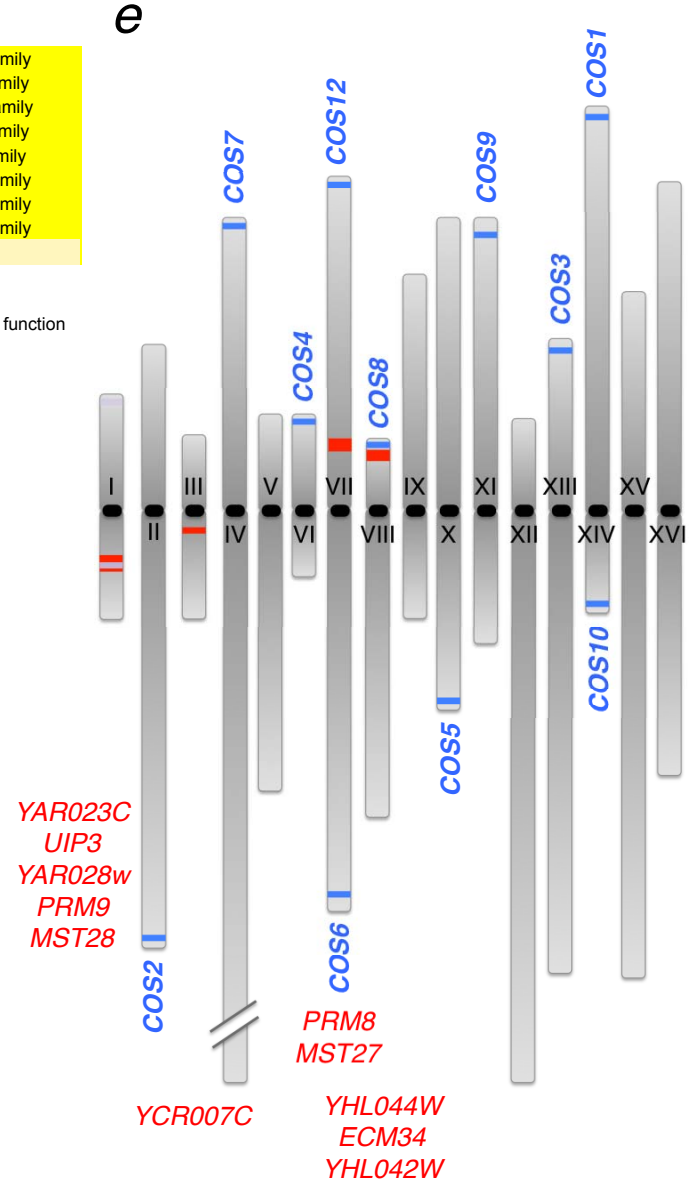

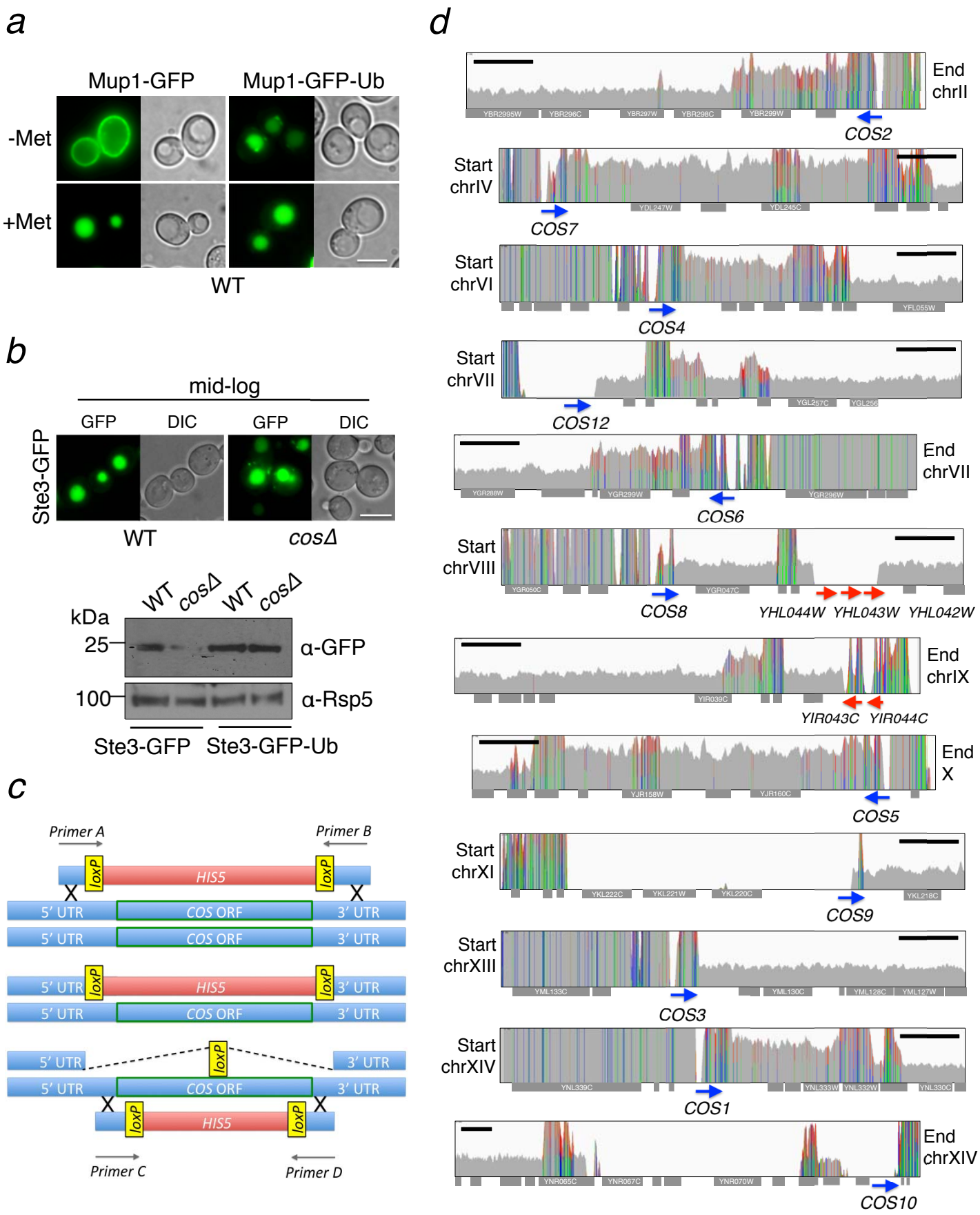
a
Mup1-GFP
Mup1-GFP-Ub
-Met
+Met
WT
b
mid-log
GFP
DIC
GFP
DIC
Ste3-GFP
WT
cosΔ
WT
cosΔ
kDa
25
α-GFP
100
α-Rsp5
Ste3-GFP
Ste3-GFP-Ub
c
Primer A
Primer B
loxP
HIS5
loxP
5′ UTR
COS ORF
3′ UTR
Primer C
Primer D
d
End chrII
COS2
Start chrIV
COS7
Start chrVI
COS4
Start chrVII
COS12
End chrVII
COS6
Start chrVIII
COS8
YHL044W
YHL043W
YHL042W
End chrIX
YIR043C
YIR044C
End X
COS5
Start chrXI
COS9
Start chrXIII
COS3
Start chrXIV
COS1
End chrXIV
COS10

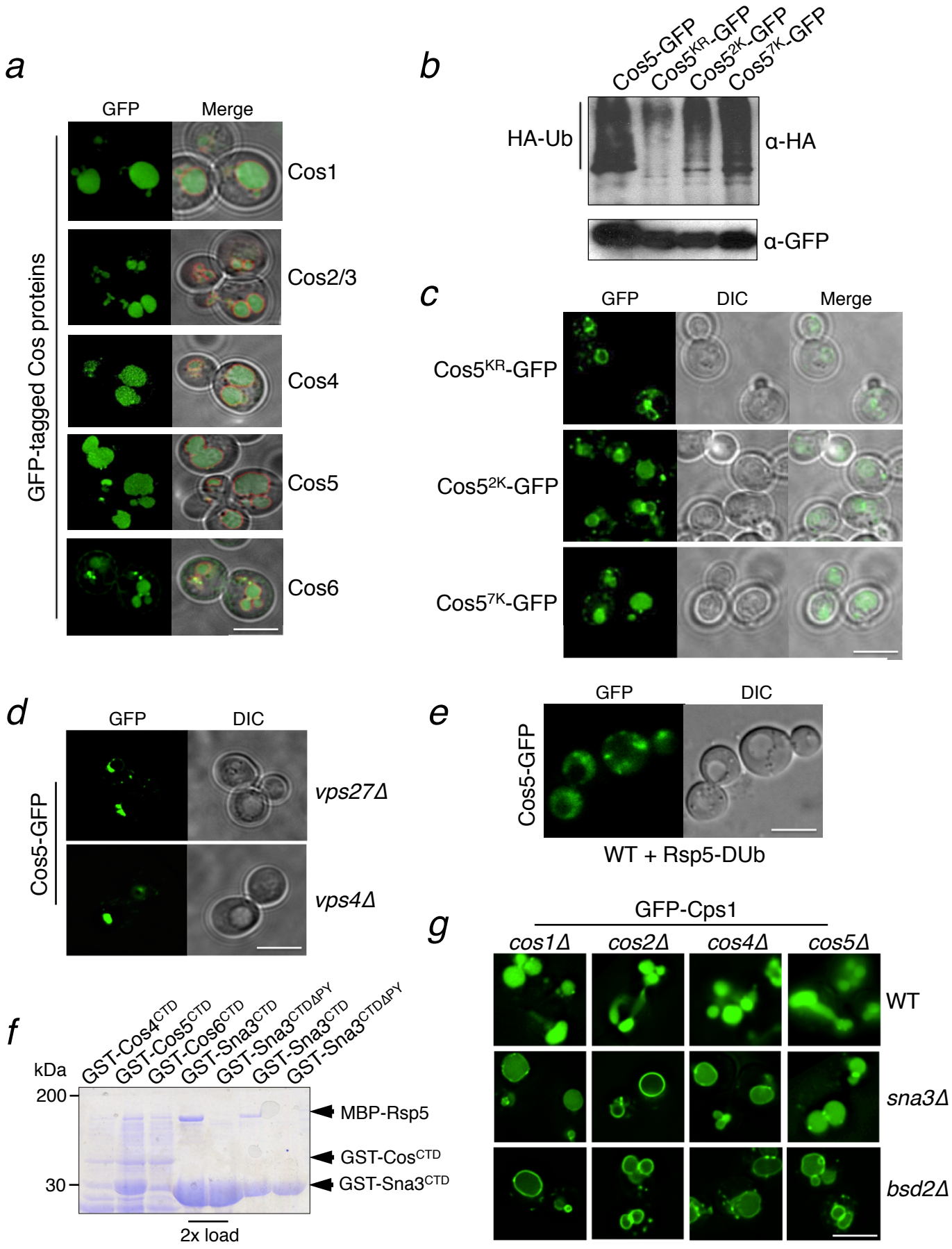
a
GFP
Merge
GFP-tagged Cos proteins
Cos1
Cos2/3
Cos4
Cos5
Cos6
b
Cos5-GFP
Cos5KR-GFP
Cos52K-GFP
Cos57K-GFP
HA-Ub
α-HA
α-GFP
c
GFP
DIC
Merge
Cos5KR-GFP
Cos52K-GFP
Cos57K-GFP
d
GFP
DIC
Cos5-GFP
vps27Δ
vps4Δ
e
GFP
DIC
Cos5-GFP
WT + Rsp5-DUb
f
kDa
GST-Cos4CTD
GST-Cos5CTD
GST-Cos6CTD
GST-Sna3CTD
GST-Sna3CTDΔPY
GST-Sna3CTD
GST-Sna3CTDΔPY
200
30
MBP-Rsp5
GST-CosCTD
GST-Sna3CTD
2x load
g
GFP-Cps1
cos1Δ
cos2Δ
cos4Δ
cos5Δ
WT
sna3Δ
bsd2Δ

Supplemental Figure 5

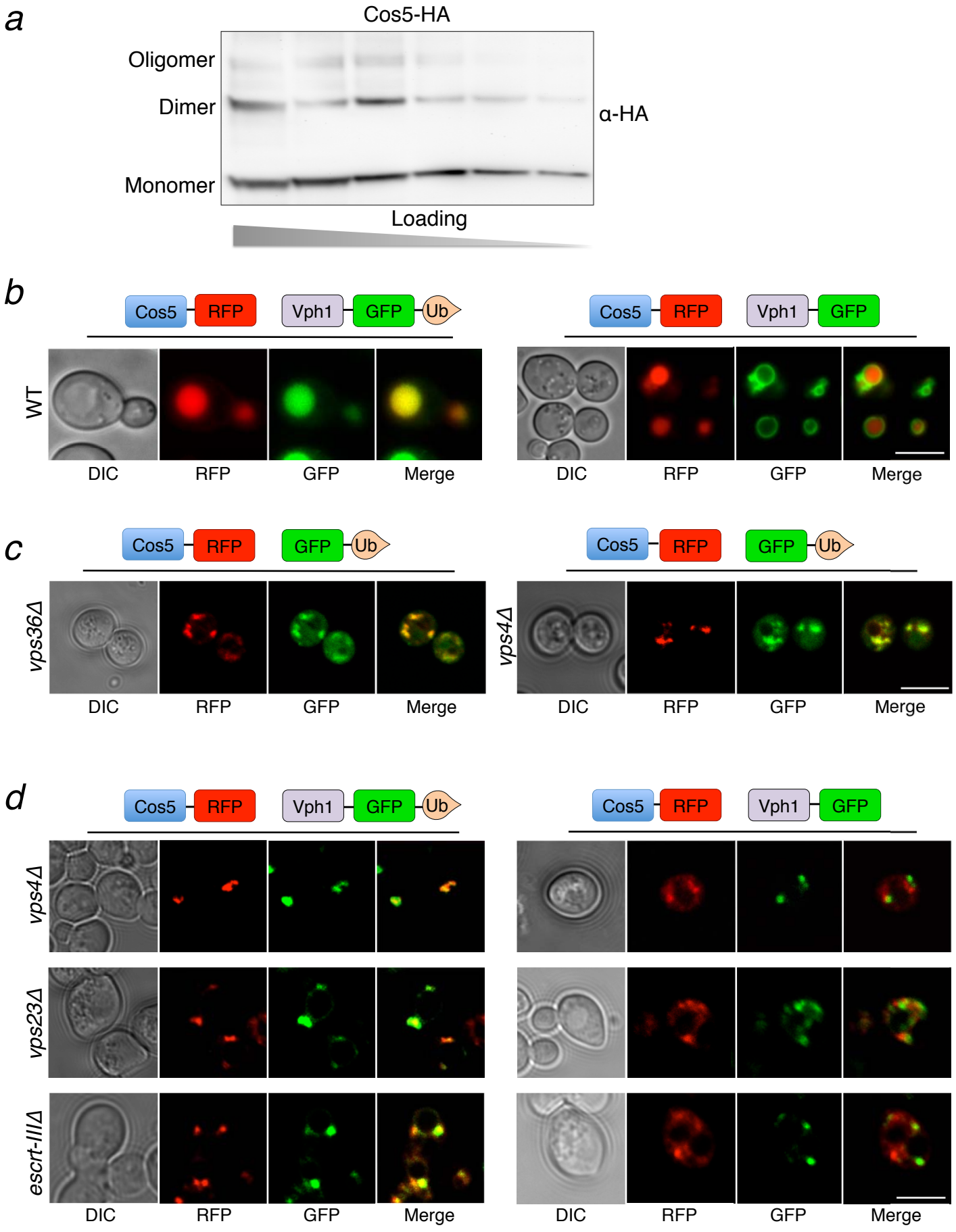

Supplemental Figure 6

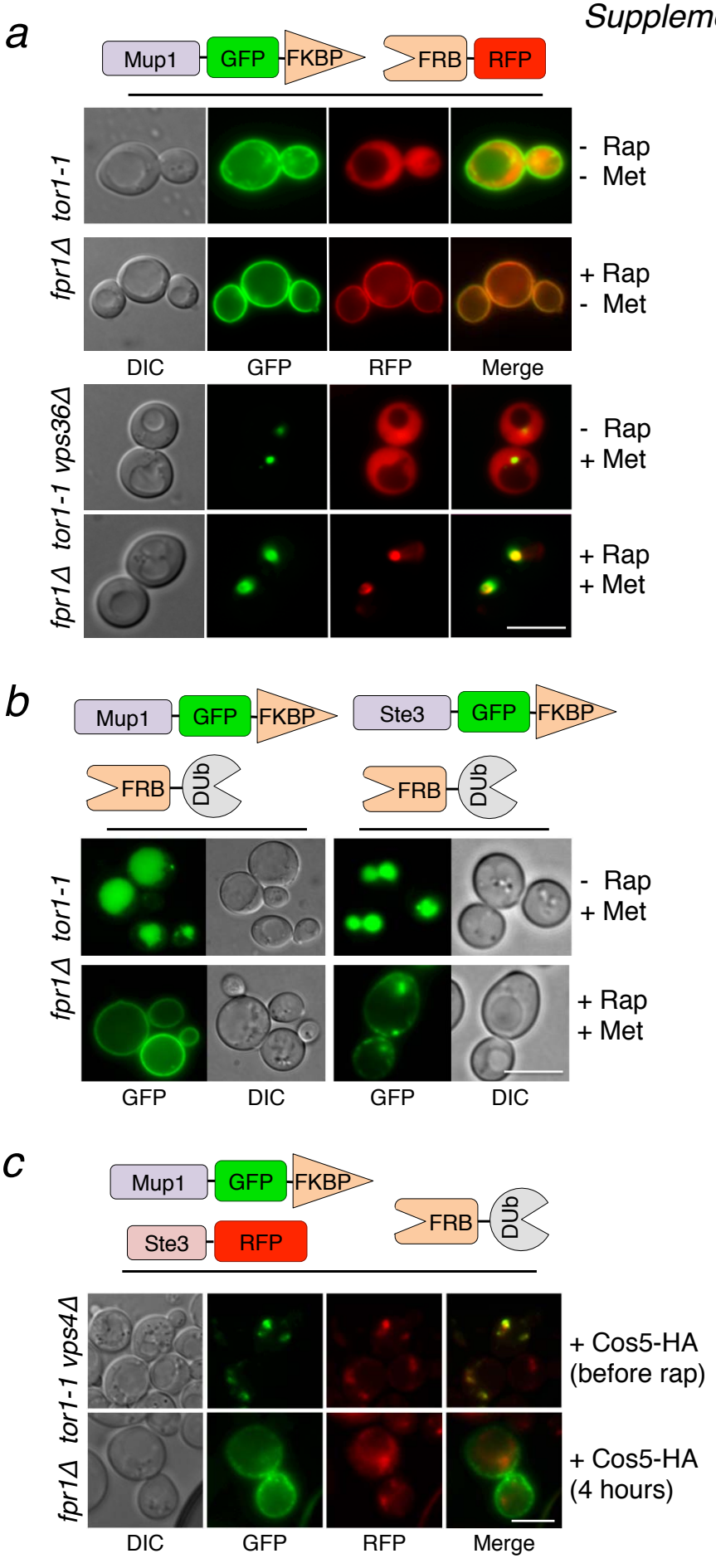

Supplemental Figure 7

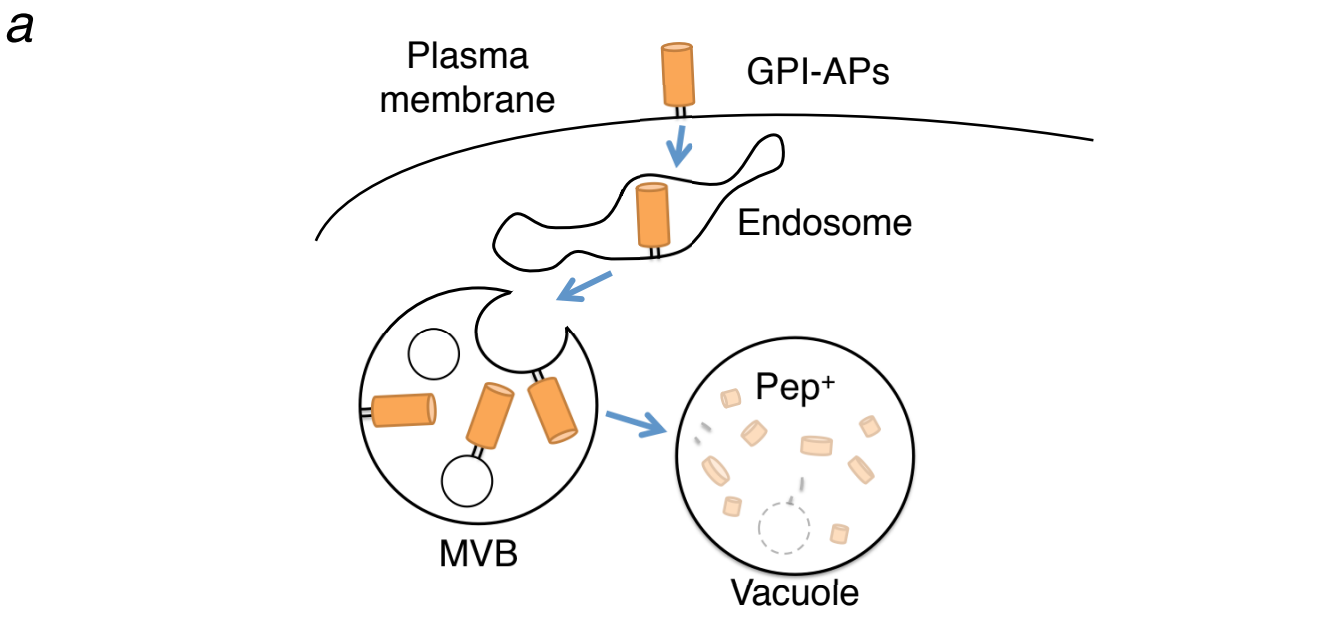

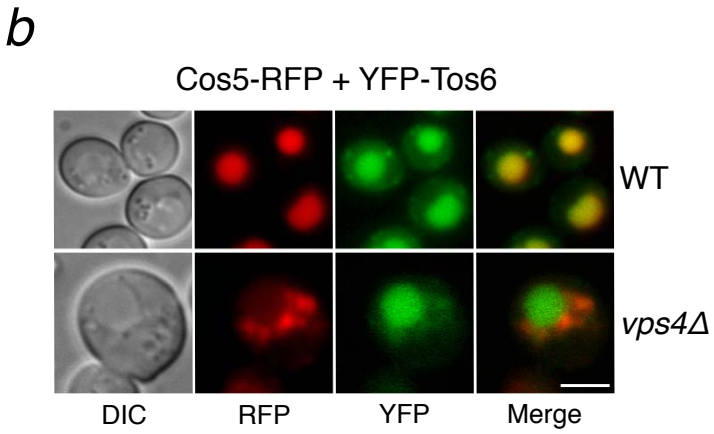

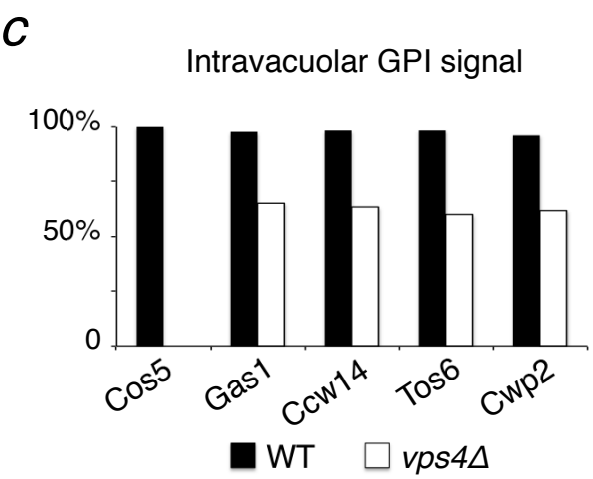

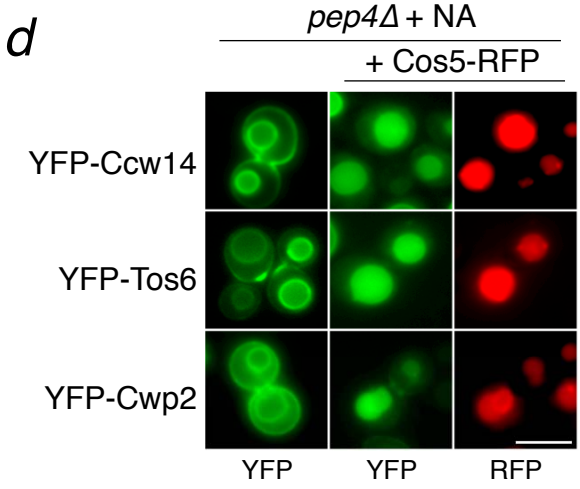

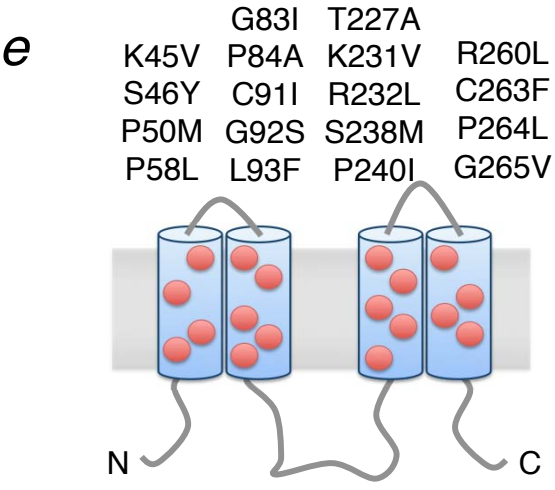

Supplementary figure legends

Figure S1, related to Figure 1: Effect of media composition, *rpd3*Δ, and *sin3*Δ on MVB sorting

a) Localization of additional GFP-tagged cargo proteins in mutant cells lacking 9 known Rsp5 adaptor proteins grown to mid- and late-log phase (OD_{600} = 1.0 and 2.0, respectively). Ste3-GFP is normally rapidly sent to the vacuole for degradation. The low levels of Ste3-GFP on the plasma membrane in cells grown to mid-log phase are absent in cells grown to late-log phase. Fur4-GFP is primarily at the cell surface in mid-log grown cells, but is completely re-localized to the vacuole in cells grown to late-log phase.

b) Cells expressing Mup1-GFP were grown to late-log phase in standard SD-Met media (2% glucose, 5 g/L ammonium sulphate, 1x vitamin base mixture), and also media that was depleted (0.5x) or supplemented (2x and 4x) with glucose, ammonium chloride, yeast nitrogen base, or buffered protons. The percentage of cells (n = indicated for each condition) showing GFP in vacuole lumen was quantified. We found changes in glucose levels and pH had no effect on Mup1-GFP sorting. Supplementing nitrogen decreased Mup1-GFP sorting to the vacuole consistent with the finding that amino acid levels control down-regulation of transporters through the TORC1 pathway (MacGurn et al., 2011). We also find the vitamin base mixture suppresses Mup1 vacuolar sorting, specifically the NAD precursor Nicotinic Acid (NA).

c) Components in Yeast Nitrogen Base, which at higher concentrations suppresses the delivery of Mup1-GFP to the vacuole when cells are grown to late-log phase.

d) GFP-Cps1 localization in wild-type cells, *rpd3*Δ and *sin3*Δ null mutant cells. Bar 5 μM.

Figure S2, related to Figure 2: *COS* gene regulation by HDACs

We found vacuolar delivery of cell surface membrane proteins could be accelerated by growth past log phase and modulated by two opposing transcription factors (accelerated by deletion of *SIR2* and attenuated by deletion of *RPD3*). These criteria were used to cross-reference existing microarray data and narrow the list of gene products that are transcriptionally activated by growth past log phase and *SIR2* deletion and repressed by *RPD3* deletion.

a) Collated microarray expression data showing gene expression profiles of the *COS* genes as cells are grown past log phase and in the indicated HDAC null mutants: *sir2Δ*, *hda1Δ, rpd3Δ* and *sin3Δ* (Bedalov et al., 2001; Bernstein et al., 2000; Gasch et al., 2000). Loss of the NAD^+-

dependent HDAC *SIR2* induces expression of many *COS* genes. Loss of *SIN3* and *RPD3*, encoding components of a NAD^+-independent HDAC complex, suppresses *COS* gene expression. Deletion of *HDA1*, another HDAC, had no affect on *COS* gene expression. The average values from duplicate experiments are displayed. The relative values are conditionally formatted, with green indicating strongest repression, red indicating strongest induction and grey as no change in expression. *COS* genes share extremely high levels of homology; it is therefore difficult to specifically generate expression profiles for each family member, for this reason average change across all *COS* genes is also shown.

b) List of the 15 genes that increase expression upon entry towards stationary phase and upon *SIR2* deletion, and decrease upon loss of *RPD3*.

c) Deletion of the HDAC gene *HDA1* has no affect on *COS* gene expression (a) or the down-regulation of Mup1-GFP to the vacuole in cultures grown to late-log phase.

d) Cos5 was chosen as a representative member of the Cos family for functional studies. Shown here are the levels of identify between *COS5* and the other family members at the deduced amino acid level (protein) and at the nucleotide level (gene), homology of which is calculated from 1000 bp upstream of the start codon to end of the ORF.

e) Schematic diagram of yeast chromosomes and the location of *COS* genes (blue) and the *DUP240* family members (red). Bar 5 μM.

Figure S3, related to Figure 3: Generation of *cos*Δ mutant cells

a) Mup1-GFP is localized to the cell surface in exponentially dividing cells but is efficiently delivered to the vacuole after 1-hour treatment with 20 μg/ml methionine. Mup1-GFP-Ub expressed in wild-type cells is found largely in the vacuole, even in cells grown in media lacking methionine.

b) Localization of Ste3-GFP in mid-log phase grown WT and *cos*Δ mutant cells. Lower, immunoblot of WT and *cos*Δ cells expressing Ste3-GFP and Ste3-GFP-Ub. Anti-GFP antibodies reveal a processed form of GFP that occurs upon cargo delivery to the vacuole lumen. The loading control with α-Rsp5 antibodies confirms no changes in the levels of Rsp5.

c) Scheme for disrupting multiple highly homologous *COS* genes. Following first round of deletion, another gene is targeted by virtue of a sequence that is no loner present in the previous deleted gene. By targeting first round of deletions with 2 selectable markers, *HIS5* from *K. lactis* and G418 resistance, each with same homology but selecting for both, therefore

confirming 2 deletions per round prior to expressing *cre*-recombinase to regenerate the selectable markers for subsequent rounds of gene disruption.

d) Genome assembly of the *cos*Δ strain showing disruption of all *COS* genes and pseudogenes. Paired-end 100 bp Illumina reads from fragmented *cos*Δ genomic DNA library were aligned separately to each of the yeast chromosomes. This artificially increases read depth at the chromosome ends that contain sequences homologous to additional loci. For instance, sequences of many of the *COS* genes can map to multiple loci. Mapping all genomic sequences to only individual chromosomes separately, however, shows unambiguous disruption of all *COS* genes. Shown are graphs of the corresponding read depths for each position, the y-axis of each graph totals 600 reads and the black bar indicates 2.5 kbp. The beginning or end of each chromosome is also labeled. The positions of the *COS* ORFs (blue arrows), *COS* pseudogenes (red arrows) as well as other annotated ORFs (grey) within the region are indicated. These data also indicate loss a few other sub-telomeric loci. However, the defects of this strain were complemented by overexpressing Cos5 from a plasmid, indicating that loss of these other regions were not responsible for the MVB sorting defects observed. Bar 5 μm.

Figure S4, related to Figure 4: Characterization of Cos proteins

a) Localization of other Cos-GFP fusion proteins in WT cells.

b) Cos5-GFP and Cos5^{KR}-GFP lacking the lysines within Cos5, were immunoprecipitated from lysates of *pep12*Δ cells also expressing HA-Ub using α-GFP antibodies. Immunoprecipitates were immunoblotted with α-GFP and α-HA. Also analyzed were Cos5^{2K}-GFP and Cos5^{7K}-GFP in which either 2 or 7 lysines were reintroduced into Cos5^{KR}-GFP.

c) Localization of Cos5^{KR}-GFP, Cos5^{2K}-GFP, Cos5^{7K}-GFP in WT cells. Introduction of novel ubiquitination sites restores MVB sorting of Cos5^{KR}-GFP.

d) Localization of Cos5-GFP in *vps27*Δ and *vps4*Δ mutants. Cos5-GFP localizes to mutant endosomal class E compartments.

e) Localization of Cos5-GFP in WT cells expressing a fusion protein of Rsp5 and the catalytic domain of the Ubp7 deubiquitinating enzyme.

f) Coomassie-stained gel of samples from the recombinant Rsp5 binding experiment in Fig. 4I. Indicated are the positions of intact GST-Cos CTD fusions, GST-Sna3 C-terminal domain fusions, and bound MBP-Rsp5.

g) Synthetic effects of deleting *SNA3* or *BSD2* and other *COS* genes on MVB sorting. Localization of GFP-Cps1 in the indicated single and double null mutants demonstrates a synthetic sorting defect between TMD containing Rsp5 adaptors Sna3 and Bsd2, and the Cos proteins.

Figure S5, related to Figure 5: Sub-compartmentalization within Endosomes

a) Immunoblot analysis of Cos5-HA expressed in *pep4*Δ cells using α-HA. The expected monomeric Cos5-HA is accompanied by a dimeric and higher order oligomeric form, which can be visualized in lanes heavily loaded with lysate.

b) Vph1-GFP-Ub is directed to the vacuolar lumen, where is co-localizes with Cos5-RFP. Also shown is the differential localization of Cos5-RFP in the vacuole and Vph1-GFP to the limiting membrane of the vacuole

c) Confocal microscopy of Cos5-RFP and GFP-Ub in mutant *vps36*Δ and *vps4*Δ cells.

d) Co-localization of Cos5-RFP and either Vph1-GFP or Vph1-GFP-Ub in the indicated class E *vps* / ESCRT mutants.

Figure S6, related to Figure 6: Characterization of the Triggered Recycling Assay

a) To demonstrate the utility of this assay we assessed the ability of Mup1-GFP-FKBP to bind FRB fusion proteins upon Rapamycin addition. Shown is localization of Mup1-GFP-FKBP and FRB-RFP in *fpr1*Δ *tor1-1* cells or *vps36*Δ *fpr1*Δ *tor1-1* cells that were treated in the absence or presence of Rapamycin (10 μM) for 90 min. Cells carried the *tor1-1* mutation allowing them to grow in the presence of Rapamycin and also lacked FKBP-12 (*fpr1*Δ) to ensure exclusive pairing of FRB-M48 to Mup1-GFP-FKBP. Cells were grown to mid-log in SD-Met media. Rapamycin induces FRB-RFP localization to Mup1-GFP-FKBP whether it is at the cell surface or trapped within class E endosomal compartments.

b) With FRB fused to M48, adding Rapamycin stabilized Mup1-GFP-FKBP at the cell surface in the presence of high concentrations of methionine [40.0 μg/ml], consistent with previous studies where Mup1-GFP was translationally fused to the UL36 DUb (Stringer and Piper, 2011). Shown is Mup1-GFP-FKBP or Ste3-GFP-FKBP were co-expressed in *fpr1*Δ *tor1-1* cells with FRB-DUb and grown in SD+Met to mid-log phase in the presence and absence of 10 μM Rapamycin.

c) Triggered recycling of Mup1-GFP-FKBP occurs more slowly in cells overexpressing Cos5-HA, as detected at the 4 hour time point in some cells. Bar = 5 μm.

Figure S7, related to Figure 7: The sorting of GPI-APs into the MVB pathway

a) Model illustrating the topology of GPI-anchored proteins as they travel through the endocytic pathway to the vacuole or to the MVB pathway. Vacuolar proteases could potentially release lumenal GFP or YFP fused onto GPI-APs regardless of whether that GPI-AP was delivered to the limiting vacuolar membrane or intralumenal vesicles derived from the MVB sorting pathway.

b) GPI-APs co-localize with Cos5-RFP in the class E compartment of *vps4*Δ (Pep^+) cells, but a large portion also accesses the lumen of the vacuole, shown by fluorescence microscopy of YFP-Tos6.

c) Intravacuolar localization of Cos5-RFP, RFP-Gas1, YFP-Ccw14, YFP-Tos6 and YFP-Cwp2 was quantified (n = >150) in wild-type and *vps4*Δ cells.

d) *pep4*Δ cells expressing YFP-labeled GPI-APs were grown to mid-log phase in media containing 100 μM NA. Localization is compared with *pep4*Δ cells co-expressing Cos5-RFP.

e) Schematic diagram of Cos5 showing membrane spanning regions (blue) and the mutations within them used to create the TMD* construct (red, residue changes labeled above). Bar = 5 μm.

Supplementary Experimental Materials

Yeast strains used in this study.

Strain	Genotype	Use	Source
BY4742	MATα *his3Δ0 leu2Δ0 lys2Δ0 ura3Δ0*	Throughout	(Brachmann et al., 1998)
SEY6210	MATα, *leu2-3,112 ura3-52 his3-Δ200 trp1-Δ901 lys2-801 suc2-Δ9*	Throughout	(Robinson et al., 1988)
		Figure 1	
ENY60	BY4742; *art1Δ art2Δ art3Δ art4Δ art6Δ art7Δ art8Δ art10Δ bsd2Δ*	1B & s1a	(Nikko and Pelham, 2009)
PLY4032	BY4742; *sir2Δ*	1D, 1E & 1F	(Winzeler et al., 1999)
PLY4033	BY4742; *rpd3Δ*	1D, 1F; s1d; 2G	(Winzeler et al., 1999)
PLY4030	BY4742; *sin3Δ*	s1d; 2G	(Winzeler et al., 1999)
		Figure 2	
JPY21	SEY6210; *mvb12Δ::HIS3*	2C	(Oestreich et al., 2007b)
PLY4031	BY4742; *hda1Δ*	s2c	(Winzeler et al., 1999)
		Figure 3	
PLY4624	BY4742; *cos1Δ cos2Δ cos3Δ cos4Δ cos5Δ cos6Δ cos7Δ cos8Δ cos9Δ cos10Δ cos12Δ yhl042wΔ yhl043wΔ yhl044wΔ yir043cΔ yir044cΔ*	3A, 3B, 3C, 3D, 3E; s2b, s2d, 7C	This study
PLY4654	BY4742; *cos1Δ cos2Δ cos3Δ cos4Δ cos5Δ cos6Δ cos7Δ cos8Δ cos9Δ cos10Δ cos12Δ yhl042wΔ yhl043wΔ yhl044wΔ yir043cΔ yir044cΔ sna3Δ*	3E	This study
		Figure 4	
LHY23	MAT**a** *leu2 ura3 his3 trp1 lys2 bar1 rsp5-1*	4A	(Dunn and Hicke, 2001)
TVY614	SEY6210; *pep4Δ::LEU2 prb1Δ::HISG prc1Δ::HIS3*	4B	(Wurmser and Emr, 1998)
PLY3983	BY4742; *sna3Δ*	4F4E?	(Winzeler et al., 1999)
PLY4359	BY4742; *bsd2Δ sna3Δ*	4F 4E?	This study
JPY130	SEY6210*; bsd2Δ::HIS3*	4F	(Lee et al., 2009)
MAY3	SEY6210; *sna3Δ::HIS3*	4F	(Oestreich et al., 2007a)
JPY489	SEY6210; *cos6Δ::HIS3*	4F	This study
JPY602	SEY6210; *bsd2Δ::HIS3 cos6Δ::*	4F	This study
JPY597	SEY6210; *cos6Δ::HIS3 sna3Δ::HIS3*	4F	This study
CBY31	SEY6210; *pep12Δ::LEU2*	4G; s4b	(Burd et al., 1997)
JPY617	SEY6210; *bsd2Δ::HIS3 pep12Δ::LEU2 sna3Δ::HIS3*	4G	This study
MBY21	SEY6210;*VPS27::HIS3*	s4d	(Shih et al., 2002)
MBY3	SEY6210; *vps4Δ::TRP1*	s4d	(Babst et al., 1997)
JPY434	SEY6210; *cos1Δ:HIS3*	s4g	This study
JPY425	SEY6210; *cos2/3Δ::HIS3*	s4g	This study
JPY435	SEY6210; *cos4Δ::HIS3*	s4g	This study
MPY1	SEY6210; *cos5Δ::HIS3*	s4g	This study
JPY590	SEY6210; *cos1Δ:HIS3 sna3Δ:HIS3*	s4g	This study
JPY592	SEY6210; *cos2/3Δ::HIS3 sna3Δ::HIS3*	s4g	This study
JPY594	SEY6210; *cos4Δ::HIS3 sna3Δ::HIS3*	s4g	This study
JPY596	SEY6210; *cos5Δ::HIS3 sna3Δ::HIS3*	s4g	This study
JPY585	SEY6210; *cos1Δ::HIS3 bsd2Δ::HIS3*	s4g	This study
JPY603	SEY6210; *cos2/3Δ::HIS3 bsd2Δ::HIS3*	s4g	This study
JPY582	SEY6210; *cos4Δ::HIS3 bsd2Δ::HIS3*	s4g	This study
JPY583	SEY6210; *cos5Δ::HIS3 bsd2Δ::HIS3*	s4g	This study
		Figure 5	
PLY4095	BY4742; *vps36Δ*	5A, 5D; s5b; 6B	(Winzeler et al., 1999)
PLY2463	SEY6210; *pep4Δ*	5B	(Macdonald et al., 2012a)
PLY4092	BY4742; *vps4Δ*	5E; s5b, s5c; 6B; s7c, s7d	(Winzeler et al., 1999)
PLY4646	BY4742; *cos1Δ cos2Δ cos3Δ cos4Δ cos5Δ cos6Δ cos7Δ cos8Δ cos9Δ cos10Δ cos12Δ yhl042wΔ yhl043wΔ yhl044wΔ yir043cΔ yir044cΔ vps4Δ*	5E	
PLY4093	BY4742; *vps23Δ*	s5c	(Winzeler et al., 1999)
PLY4348	BY4742; *did2Δ vps60Δ vps2Δ vps20Δ vps24Δ snf7Δ*	s5c; 6B	This study

		Figure 6	
PLY4168	BY4742; *vps24Δ*	6A, 6B	(Winzeler et al., 1999)
PLY4169	BY4742; *snf7Δ*	6A, 6B	(Winzeler et al., 1999)
W303	MATα *ade 2-1 trp1-1 can1-100 leu2-3,112 his3-11,15 ura3*		(Thomas and Rothstein, 1989)
KY14708	W303; *tor1-1 fpr1Δ*	s6b	(Haruki et al., 2008)
PLY4575	W303; *tor1-1 fpr1Δ vps4Δ CUP1-HA-FRB-M48 MUP1-GFP-FKBP*	6D	This study
PLY4392	W303; *tor1-1 fpr1Δ vps36Δ* (W303)	s6a	This study
		Figure 7	
PLY2030	BY4742; *pep4Δ*	7A, 7C, 7D; s7b, s7e	(Winzeler et al., 1999)
PLY4099	SEY6210; *pep4Δ vps4Δ*	7B	(Macdonald et al., 2012a)
PLY4648	BY4742; *cos1Δ cos2Δ cos3Δ cos4Δ cos5Δ cos6Δ cos7Δ cos8Δ cos9Δ cos10Δ cos12Δ yhl042wΔ yhl043wΔ yhl044wΔ yir043cΔ yir044cΔ pep4Δ::LEU2 atg8Δ::KanMX*	3F, 3H, 7E, 7F, 7G	This study

Plasmids used in this study.

Plasmid	Description	Use	Source
pRS413	Low copy yeast shuttle plasmid containing *HIS3* marker	Throughout	(Sikorski and Hieter, 1989)
pRS415	Low copy yeast shuttle plasmid containing *LEU2* marker	Throughout	(Sikorski and Hieter, 1989)
pRS416	Low copy yeast shuttle plasmid containing *URA3* marker	Throughout	(Sikorski and Hieter, 1989)
		Figure 1	
pCHL642	pRS416 expressing Mup1-GFP from *MUP1* promoter	1A, 1B, 1C, 1D, 1E, 1F; s1b; 2F, 2G; s2c; 3A; s3a, 4C; 6B	(Lin et al., 2008)
pCHL571	pRS416 expressing Can1-GFP from *CAN1* promoter	1B	(Lin et al., 2008)
pPL5633	pRS416 expressing Yor1-GFP from *CUP1* promoter	1B	This study
pPL2583	pRS416 expressing GFP-Snc1 from *TPI1* promoter	1B; 3D	(Burston et al., 2009)
pPL967	pRS415 expressing Ste3-GFP from *STE3* promoter	s1a; s3b; 6A	(Urbanowski and Piper, 2001)
pPL3797	pRS415 expressing Fur4-GFP from *CUP1* promoter	s1a	(Stringer and Piper, 2011)
pPL2356	pRS416 expressing GFP-Cps1 from *TPI1* promoter	s1d	(Reggiori and Pelham, 2001)
		Figure 2	
pMA27	pRS416 expressing Cos5-GFP from *TDH3* promoter	2C, 4A, 4B, 4E, 4G; s4a, s4d, s4e	This study
pPL5000	pRS416 expressing Cos5-HA from *CUP1* promoter	2D, 2E, 2F, 2G; 3D, 3E, 4D, 5B, 6A, 6B	This study
		Figure 3	
pPL4147	pRS415 expressing Mup1-GFP-Ub from *CUP1* promoter	3A, 3B, s3a	(Stringer and Piper, 2011)
pPL5696	pRS416 expressing Mup1-GFP-Ub-Ub from *CUP1* promoter	3B	This study
pPL3878	pRS415 expressing GFP-Ub from *PRC1* promoter	3C, s5b	(Bilodeau et al., 2003)
pPL2279	pRS415 expressing $Sna3^{KR}$ from *SNA3* promoter Sna3 (K19R, K125R)	3E	(MacDonald et al., 2012b)
pPL3484	pRS415 expressing Ste3-GFP-Ub from *STE3* promoter	s3b	(Bilodeau et al., 2003)

		Figure 4	
pMA131	pGPD416-Cos5^{KR}-GFP	4A, 4B; s4c	This study
pPL5103	pRS416 expressing Cos5-GFP-UL36 from *CUP1* promoter	4A	This study
pPL5003	pRS416 expressing Cos5^{KR}-HA from *CUP1* promoter	4D; 5B	This study
pPL5764	pRS416 expressing Cos5^{KR}-HA-myc-Ub from *CUP1* promoter	4D	This study
pGO45	pRS426-GFP-Cps1	4F; s4g	(Odorizzi et al., 1998)
pGPD414HA-Ub	pRS414 expressing HA-Ub	4G; s4b	(Oestreich et al., 2007a)
pJP10	GST-Cos4^{CTD2}(Cos 4 residues 297-380)	4I; s4f	This study
pJP21	GST-Cos5^{CTD2}(Cos5 residues 299-384)	4I; s4f	This study
pJP25	GST-Cos6^{CTD2}(Cos6 residues 299-382)	4I; s4f	This study
GST-Sna3^{CTD}	GST-Sna3^{CTD}	4I; s4f	(Oestreich et al., 2007a)
GST-Sna3$^{CTD\Delta PY}$	GST-Sna3$^{CTD\Delta PY}$	4I; s4f	(Oestreich et al., 2007a)
pJL242	His-MBP-Rsp5^{WT}	4I; s4f	(Oestreich et al., 2007a)
pMA24	pGPD416-Cos1-GFP	s4a	This study
pMA25	pGPD416-Cos2/3-GFP	s4a	This study
pMA26	pGPD416-Cos4-GFP	s4a	This study
pMA27	pGPD416-Cos5-GFP	s4a	This study
pMA28	pGPD416-Cos6-GFP	s4a	This study
pMA132	pGPD416-Cos5^{2K}-GFP	s4c	This study
pMA133	pGPD416-Cos5^{7K}-GFP	s4c	This study
pPL3742	pRS416 expressing Rsp5-Ubp7-3xHA Active Ubp7 (catalytic domain)	s4e, 7A	(Stringer and Piper, 2011)
pPL5128	pRS415 expressing Cos5-GFP from *TDH3* promoter	s4e	This study
		Figure 5	
pPL5392	pRS416 expressing Cos5-mCherry-GFP from *CUP1* promoter	5A	This study
pPL5390	pRS416 expressing Cos5-mCherry from *CUP1* promoter	5A; s5b; 7G, 7H	This study
pPL5128	pRS415 expressing Cos5-GFP from *TDH3* promoter	5A, 5D; 7B, 7F; s7c, s7d, s7e	This study
pPL5424	pRS415 expressing Cos5-mCherry from *CUP1* promoter	5A; s5a, s5c	This study
pPL1556	pRS416 expressing Vph1-GFP-Ub from *VPH1* promoter	5A, 5D, 5E; s5a, s5c	(Urbanowski and Piper, 2001)
pPL848	pRS416 expressing Vph1-GFP from *VPH1* promoter	5D, 5E; s5a, s5c	(Urbanowski and Piper, 2001)
pPL4147	pRS416 expressing Mup1-mCherry-Ub from *CUP1* promoter	5E	(Stringer and Piper, 2011)
		Figure 6	
pPL5519	pRS416 expressing Cos5-HA from *TEF1* promoter	6C, 6D; s6c	This study
pPL3607	pRS416 expressing Ste3-mCherry from *STE3* promoter	6D; s6c	(Ren et al., 2008)
pPL5348	pRS-*ADE2* expressing Mup1-GFP-FKBP from *CUP1* promoter	s6a, s6b	This study
pPL5011	pRS416 expressing HA-FRB-mCherry from *SNA3* promoter	s6a	This study
pPL5350	pRS-*ADE2* expressing Ste3-GFP-FKBP from *CUP1* promoter	s6b	This study
		Figure 7	
p416VenusCcw14	pRS416 expressing Venus-Ccw14 from *ADH1* promoter	7A, 7E, 7F; s7b, s7d, s7e	(Castillon et al., 2009)
p416VenusTos6	pRS416 expressing Venus-Tos6 from *ADH1* promoter	7B, 7F; s7c, s7d, s7e	(Castillon et al., 2009)
p416HA-GAS1	pRS416 expressing HA-Gas1 from *GAS1* promoter	7C, 7E, 7G	Scott Moye-Rowley
pPL5724	pRS416 expressing Myc-Sed1 from *MET25* promoter, contains the 20 residue N-terminal Alpha factor signal sequence	7C	This study
pPL5692	pRS416 expressing Myc-Rot1 from *MET25* promoter, contains the 20 residue N-terminal Alpha factor signal sequence	7D	This study
pPL5268	pRS415 expressing Cos5-HA from *CUP1* promoter	7E	This study
p416VenusCwp2	pRS416 expressing Venus-Cwp2 from *ADH1* promoter	7E, 7F; s7b, s7d, s7e	(Castillon et al., 2009)
pPL5742	pRS415 expressing Cos5-TMD*-mCherry from *CUP1* promoter (K45V, S46Y, P50M, P58L, G83I, P84A, C91I, G92S, L93F, T227A, K231V, R232L, S238M, P240I, R260L, C263F, P264L, G265V	7G	This study
pPL5720	pRS416 expressing Cos5-TMD*-mCherry from *CUP1* promoter (K45V, S46Y, P50M, P58L, G83I, P84A, C91I, G92S, L93F, T227A, K231V, R232L, S238M, P240I, R260L, C263F, P264L, G265V	7H	This study
pPL5707	pRS413 expressing Venus-Ccw14 from *ADH1* promoter	7H	This study

Supplementary Experimental Procedures

Generation of the cosΔ null strain

The *COS* gene family, *COS1* – *COS10* and *COS12*, are encoded exclusively in sub-telomeric regions that share regions of high homology. The strategy to delete the entire family of *COS* related genes involved several technical considerations due to this high level of homology between different *COS* loci, not only within the open reading frame (ORF) but also extending far into the 5' and 3 untranslated regions (UTRs). We designed a nested gene disruption strategy to non-specifically delete *COS* genes, whereby progressively smaller integration cassettes are used to target *only* the remaining *COS* genes. Disruption cassettes that confer resistance to G418 (*kanMX*) and histidine prototrophy (*HIS5*) were sequentially integrated at 2 loci and yeast selected for both markers prior to expression of *cre*-recombinase to recycle the markers for further rounds of disruption.

Every cassette integration, and subsequent *loxP* recombination, was confirmed by PCR analysis of isolated genomic DNA (gDNA). The homology between different *COS* genes was so high that even short oligonucleotides, to confirm loci had been correctly modified, could not distinguish between certain pairs of *COS* genes (*COS1* & *COS4*, *COS2* & *COS6*, *COS5* & *COS7*). For this reason, these pairs were never targeted in the same round of *KanMX* and *HIS5* integrations. Instead, one of the genes was targeted first and converted to a *loxP* site before the remaining gene was disrupted.

We found integrations that remove large regions of the telomeres were unsuccessful, possibly because such deletions prove lethal. To avoid this, we used a gene disruption strategy where the *COS* promoter sequence, the start codon and a portion of the ORF were replaced with a *loxP* marked cassette. The insertion was designed to leave a *loxP* scar containing a stop codon and shifting the frame of the remaining ORF following Cre-recombinase activity. The largest of the non-specific cassettes targeted ~150 bp of 5' promoter sequence and ~500 bp of the ORF; the smallest cassette targeted ~100 bp of 5' promoter sequence and ~250 bp of the ORF.

It was difficult to avoid targeting the 2 reported *COS* pseudogenes (*YHL042* / *YHL043W* / *YHL044W* and *YIR04C* / *YIR044C*) using our generalized strategy, so we also disrupted these loci. Although these loci are denoted as pseudogenes in the reference genome of strain S288c, it remains unclear whether these loci truly do not encode functional proteins. The *DUP380* locus

YHL043W is reported to be a non-functional pseudogene due to the insertion of a frame shifting nucleotide approximately half way through the ORF. However, many strains sequenced and documented in the *Saccharomyces* Genome database (SGD) do not report this insertion and report a *bona fide* and un-assigned member of the *COS* gene family. Less sequence data is available for *YIR044C* to define stop codon insertion frequency. However, the sequence identity of the *YIR04C / YIR044C* is extremely similar to the *COS* gene consensus and is denoted only as a pseudogene on account of a single nucleotide insertion that prematurely encodes termination.

Pulse-chase analysis

Pulse-chase analysis of Cos5-GFP and Cos5^{KR}-GFP was performed using methods as previously described (Babst et al., 2002). Cos5 was detected with monoclonal anti-GFP AV-JL8 (Clontech). Quantitation was performed using phosphorimaging screens and a Storm 84 System (GE Healthcare, Little Chalfont, Buckinghamshire, United Kingdom).

In vitro binding studies

Expression and purification of Rsp5 recombinant proteins and immunoprecipitation and in vitro binding experiments were performed as described previously (Lee et al., 2009). BL21 *E.coli* (Stratagene) expressing His-MBP-Rsp5 and GST- Cos4^{ctd}, GST- Cos5^{ctd2}, GST- Cos6^{ctd2}, GST-Sna3^{ctd}, GST- Sna3$^{ctd\Delta py}$ constructs were induced with 0.5mM IPTG at 37^0 for 4 hours, lysed and stored at -80^{0}C. Binding studies were performed as previously described in (Oestreich et al., 2007a). Samples were subjected to SDS-PAGE and Western blotting. Binding to His-MBP-Rsp5 was detected with monoclonal anti-MBP (Sigma).

Bafilomycin induced sorting of GPI-APs

During the course of these studies we discovered that the V-ATPase inhibitor Bafilomycin enhanced GPI-AP sorting to the vacuole, albeit through an unknown mechanism. We typically add 1 μM Bafilomycin to yeast cells grown in minimal media and find this is sufficient to rapidly direct GPI-APs into the vacuole, as measured by both intravacuolar delivery of fluorescently tagged proteins expressed in *pep4*Δ cells by microscopy and enhanced degradation of total protein levels shown by immunoblot.

Supplementary References

Babst, M., Katzmann, D.J., Snyder, W.B., Wendland, B., and Emr, S.D. (2002). Endosome-associated complex, ESCRT-II, recruits transport machinery for protein sorting at the multivesicular body. Dev Cell *3*, 283-289.

Babst, M., Sato, T.K., Banta, L.M., and Emr, S.D. (1997). Endosomal transport function in yeast requires a novel AAA-type ATPase, Vps4p. EMBO J *16*, 1820-1831.

Bedalov, A., Gatbonton, T., Irvine, W.P., Gottschling, D.E., and Simon, J.A. (2001). Identification of a small molecule inhibitor of Sir2p. Proc Natl Acad Sci USA *98*, 15113-15118.

Bernstein, B.E., Tong, J.K., and Schreiber, S.L. (2000). Genomewide studies of histone deacetylase function in yeast. Proc Natl Acad Sci USA *97*, 13708-13713.

Bilodeau, P.S., Winistorfer, S.C., Kearney, W.R., Robertson, A.D., and Piper, R.C. (2003). Vps27-Hse1 and ESCRT-I complexes cooperate to increase efficiency of sorting ubiquitinated proteins at the endosome. J Cell Biol *163*, 237-243.

Brachmann, C.B., Davies, A., Cost, G.J., Caputo, E., Li, J., Hieter, P., and Boeke, J.D. (1998). Designer deletion strains derived from Saccharomyces cerevisiae S288C: a useful set of strains and plasmids for PCR-mediated gene disruption and other applications. Yeast *14*, 115-132.

Burd, C.G., Peterson, M., Cowles, C.R., and Emr, S.D. (1997). A novel Sec18p/NSF-dependent complex required for Golgi-to-endosome transport in yeast. Mol Biol Cell *8*, 1089-1104.

Burston, H.E., Maldonado-Baez, L., Davey, M., Montpetit, B., Schluter, C., Wendland, B., and Conibear, E. (2009). Regulators of yeast endocytosis identified by systematic quantitative analysis. J Cell Biol *185*, 1097-1110.

Castillon, G.A., Watanabe, R., Taylor, M., Schwabe, T.M., and Riezman, H. (2009). Concentration of GPI-anchored proteins upon ER exit in yeast. Traffic *10*, 186-200.

Dunn, R., and Hicke, L. (2001). Domains of the Rsp5 ubiquitin-protein ligase required for receptor-mediated and fluid-phase endocytosis. Mol Biol Cell *12*, 421-435.

Gasch, A.P., Spellman, P.T., Kao, C.M., Carmel-Harel, O., Eisen, M.B., Storz, G., Botstein, D., and Brown, P.O. (2000). Genomic expression programs in the response of yeast cells to environmental changes. Mol Biol Cell *11*, 4241-4257.

Haruki, H., Nishikawa, J., and Laemmli, U.K. (2008). The anchor-away technique: rapid, conditional establishment of yeast mutant phenotypes. Mol Cell *31*, 925-932.

Lee, J.R.E., Oestreich, A.J., Payne, J.A., Gunawan, M.S., Norgan, A.P., and Katzmann, D.J. (2009). The HECT domain of the ubiquitin ligase Rsp5 contributes to substrate recognition. J Biol Chem *284*, 32126-32137.

Lin, C.H., MacGurn, J.A., Chu, T., Stefan, C.J., and Emr, S.D. (2008). Arrestin-related ubiquitin-ligase adaptors regulate endocytosis and protein turnover at the cell surface. Cell *135*, 714-725.

Macdonald, C., Buchkovich, N.J., Stringer, D.K., Emr, S.D., and Piper, R.C. (2012a). Cargo ubiquitination is essential for multivesicular body intralumenal vesicle formation. EMBO Rep *13*, 331-338.

MacDonald, C., Stringer, D.K., and Piper, R.C. (2012b). Sna3 Is an Rsp5 Adaptor Protein that Relies on Ubiquitination for Its MVB Sorting. Traffic.

MacGurn, J.A., Hsu, P.-C., Smolka, M.B., and Emr, S.D. (2011). TORC1 regulates endocytosis via Npr1-mediated phosphoinhibition of a ubiquitin ligase adaptor. In Cell, pp. 1104-1117.

Nikko, E., and Pelham, H.R. (2009). Arrestin-mediated endocytosis of yeast plasma membrane transporters. Traffic *10*, 1856-1867.

Odorizzi, G., Babst, M., and Emr, S.D. (1998). Fab1p PtdIns(3)P 5-kinase function essential for protein sorting in the multivesicular body. Cell *95*, 847-858.

Oestreich, A.J., Aboian, M., Lee, J., Azmi, I., Payne, J., Issaka, R., Davies, B.A., and Katzmann, D.J. (2007a). Characterization of multiple multivesicular body sorting determinants within Sna3: a role for the ubiquitin ligase Rsp5. Mol Biol Cell *18*, 707-720.

Oestreich, A.J., Davies, B.A., Payne, J.A., and Katzmann, D.J. (2007b). Mvb12 is a novel member of ESCRT-I involved in cargo selection by the multivesicular body pathway. Mol Biol Cell *18*, 646-657.

Reggiori, F., and Pelham, H.R. (2001). Sorting of proteins into multivesicular bodies: ubiquitin-dependent and -independent targeting. EMBO J *20*, 5176-5186.

Ren, J., Pashkova, N., Winistorfer, S., and Piper, R.C. (2008). DOA1/UFD3 plays a role in sorting ubiquitinated membrane proteins into multivesicular bodies. J Biol Chem *283*, 21599-21611.

Robinson, J.S., Klionsky, D.J., Banta, L.M., and Emr, S.D. (1988). Protein sorting in Saccharomyces cerevisiae: isolation of mutants defective in the delivery and processing of multiple vacuolar hydrolases. Mol Cell Biol *8*, 4936-4948.

Shih, S.C., Katzmann, D.J., Schnell, J.D., Sutanto, M., Emr, S.D., and Hicke, L. (2002). Epsins and Vps27p/Hrs contain ubiquitin-binding domains that function in receptor endocytosis. Nat Cell Biol *4*, 389-393.

Sikorski, R.S., and Hieter, P. (1989). A system of shuttle vectors and yeast host strains designed for efficient manipulation of DNA in Saccharomyces cerevisiae. Genetics *122*, 19-27.

Stringer, D.K., and Piper, R.C. (2011). A single ubiquitin is sufficient for cargo protein entry into MVBs in the absence of ESCRT ubiquitination. J Cell Biol *192*, 229-242.

Thomas, B.J., and Rothstein, R. (1989). Elevated recombination rates in transcriptionally active DNA. Cell *56*, 619-630.

Urbanowski, J.L., and Piper, R.C. (2001). Ubiquitin sorts proteins into the intralumenal degradative compartment of the late-endosome/vacuole. Traffic *2*, 622-630.

Winzeler, E.A., Shoemaker, D.D., Astromoff, A., Liang, H., Anderson, K., Andre, B., Bangham, R., Benito, R., Boeke, J.D., Bussey, H.*, et al.* (1999). Functional characterization of the S. cerevisiae genome by gene deletion and parallel analysis. Science *285*, 901-906.

Wurmser, A.E., and Emr, S.D. (1998). Phosphoinositide signaling and turnover: PtdIns(3)P, a regulator of membrane traffic, is transported to the vacuole and degraded by a process that requires lumenal vacuolar hydrolase activities. EMBO J *17*, 4930-4942.